USE OF NANOINDENTATION AND SILVISCAN TO DETERMINE THE MECHANICAL PROPERTIES OF 10 HARDWOOD SPECIES

Yan Wu

PhD Student
Nanjing Forestry University
Nanjing, China
Visiting Scholar
University of Tennessee

Siqun Wang*†

Associate Professor
Tennessee Forest Products Center
University of Tennessee
2506 Jacob Drive, Ag. Campus
Knoxville, TN 37996-4570

Dingguo Zhou

Professor
College of Wood Science & Technology
Nanjing Forestry University
Nanjing, China

Cheng Xing

Postdoctoral Research Associate
Tennessee Forest Products Center
University of Tennessee
2506 Jacob Drive, Ag. Campus
Knoxville, TN 37996-4570

Yang Zhang

Professor
College of Wood Science & Technology
Nanjing Forestry University
Nanjing, China

(Received July 2008)

Abstract.   The objectives of this study were to investigate the properties of bulk wood and cell walls of 10 hardwoods, Alder Birch (*Betula* spp.), Asian White Birch (*Betula platyphylla* spp.), Manchurian Ash (*Fraxinus mandshurica* spp.), Mongolian Oak (*Quercus* spp.), Poplar (*Populus* spp.), Red Oak (*Quercus* spp), White Oak (*Quercus* spp.), Iroko (*Chlorophora excelsa* spp.), Keranji (*Dialium* spp.), and *Kwila* (Intsia spp.). The relationship between wood species and mechanical properties as well as the relativity of wood species and microfibril angle to the hardness and elastic modulus were investigated. It showed that lower density hardwoods had higher microfibril angle than higher density hardwoods. The elastic moduli of bulk wood and cell walls of wood were both significantly different, whereas the hardness of the cell wall was not significantly different among the 10 species. The SilviScan elastic modulus increased with wood density and decreased with microfibril angle. At the cell wall level, the elastic modulus and hardness obtained by nanoindentation

* Corresponding author: swang@utk.edu
† SWST member

were more related to the properties of natural libriform fibers. However, there was no significant trend found for the hardness of the cell wall as affected by either wood bulk density or microfibril angle.

Keywords: Elastic modulus, hardness, mechanical properties, microfibril angle, nanoindentation, SilviScan, wood density.

INTRODUCTION

Wood is a cellular solid characterized by a high degree of anisotropy at all levels of structures. It consists of different cell types that are oriented in an axial direction (tracheids in softwood and libriform, tracheid fibers, and vessels in hardwood) or in a radial direction (ray cells). The cell walls of wood fibers are built up of layers of different thicknesses. Each layer has different spiral microfibril angles (MFA) and chemical components. The secondary cell wall layer (S_2) is an important factor that determines the mechanical properties of the fiber because its thickness accounts for approximately 80% of the entire cell wall thickness (Fengel and Stoll 1973). The stiffness of wood mostly relies on the semicrystalline cellulose microfibril as found in a Z-helix form around the lumen within the cell walls of wood (Meylan and Butterfield 1978) as well as its microfibril angle (Jentzen 1964; Cave 1968; Gordon and Jeronimidis 1980; Tze et al 2007).

Microfibril angle has been considered an important factor that determines wood properties such as stiffness and strength and it has been shown by Cave (1968, 1969) that longitudinal elastic modulus (stiffness) of wood is very much dependent on S_2 microfibril angle. On the one hand, conventional wisdom indicates that as the microfibril angle increases (to a value up to 90°), the longitudinal stiffness would decrease (Tze et al 2007). On the other hand, wood bulk density is also strongly related to the mechanical properties of wood (Cown et al 1999; Evans and Ilic 2001). A linear relationship between hardness and wood bulk density was reported in some articles (Ylinen 1943; Miyajima 1963; Kollman and Côté 1968; Holmberg 2000). Higher density hardwood species generally exhibit higher static bending modulus of elasticity as reported by the Forest Products Laboratory (1999) and Cheng et al (1992) in Table 1.

During recent years, several developments have taken place in biotechnology, including genetic tree improvement. Characterizing wood quality quickly and reliably becomes more important for evaluating whether the genetic application is successful. The recent development of SilviScan-2 (Evans 1997, 1999) has provided a tool to conduct the rapid scanning of increment cores for tree improvement programs and large-scale resource assessment. SilviScan provides pith-to-bark measurements of fiber width, wood density, and microfibril angle. From these data, fiber wall thickness, coarseness, and wood stiffness can be estimated.

Wood is a natural composite material with the cellulose fibrils acting as reinforcing elements in an amorphous matrix of hemicellulose and lignin. The mechanical behavior of the elementary cells (fibers) is related to the cell wall structure and the mechanical properties of the constituents (Nilsson and Gustafsson 2007).

Many researchers in wood science are critically considering the effective use of natural fibers for composite manufacture, suggesting those as a viable alternative fiber to replace conventional fibers (Mohanty et al 2001; Keller 2003; Shibata

Table 1. *Mechanical properties of some hardwood species.*

Hardwood species	Specific gravity[a]	Static bending MOE (GPa)
Poplar	0.391 – 0.540	6.90 – 11.4
Birch	0.597 – 0.690	9.20 – 14.1
Red Oak	0.610 – 0.690	11.3 – 15.7
Iroko	0.620 – 0.720	9.38 – 9.40
White Oak	0.630 – 0.720	7.10 – 14.1
Manchurian Ash	0.643 – 0.680	12.9 – 14.6
Mongolian Oak	0.748 – 0.760	13.2 – 15.5
Kwila	0.725 – 0.940	16.0 – 18.0
Keranji	0.755 – 1.250	16.7 – 21.1

[a] Oven-dry mass/green volume basis.

Data of Red Oak and White Oak from Forest Products Laboratory (1999); Iroko, Kwila and Keranji from Chudnoff (1979) and Cheng et al (1992); others from Cheng et al (1992).

et al 2004; Zini et al 2004; Cheng et al 2007). Therefore, a better understanding of the properties and characteristics of natural fibers, more specifically, testing of the mechanical properties of the cell wall S_2 layer, will be helpful to the manufacture of biocomposites and lignocellulosic fiber-reinforced composites (Lee et al 2007; Tze et al 2007; Xing et al 2008, 2009).

In the manufacture of biocomposites and natural fiber-reinforced composites, it is critical to understand the mechanical properties of wood fibers (Wang et al 2006). Nanoindentation is a technique that is used to determine the mechanical properties of a material at the submicron or nanoscale. The test involves penetration of a sample material using an indenter, whereas the penetration depth and load are recorded so that the relative elastic modulus and hardness of the material at the indented location can be subsequently calculated. With the use of nanoindentation, it is possible to determine more precisely the effect of the mechanical properties of fiber cell wall on the entire wood in different wood species.

Some wood scientists have investigated the nanomechanical properties of wood cell walls by nanoindentation, but they all focused on their local softwood species such as loblolly pine (Tze et al 2007; Xing et al 2008, 2009) and spruce (Gindl and Schöberl 2004; Jiang et al 2004). No reference was found for determination of the nanomechanical properties of hardwood by nanoindentation. Compared with softwood, hardwood species have more complex wood structure and cellular compositions. About 90 – 95% of the wood cells in softwood are tracheids; however, in hardwood, other than fiber tracheids, the number of vessels is also high (Yin 1996). The volume fraction of vessels plays an important role in determining hardwood density and mechanical properties. However, whether the mechanical properties of the fiber cell wall contribute to the bulk wood strength and whether the higher strength (or higher density) of bulk wood consist of a stronger fiber cell wall are still unclear. Therefore, the objective of this study was to investigate the

mechanical properties of the fiber cell wall in 10 hardwoods with density varying from 410 – 1180 kg/m^3 by nanoindentation and SilviScan as affected by wood species (density) and MFA.

MATERIALS AND METHODS

Sample Preparation

Seven hardwood samples, Alder Birch (*Betula* spp.), Asian White Birch (*Betula platyphylla* spp.), Iroko (*Chlorophora excelsa* spp.), Keranji (*Dialium* spp.), Kwila (*Intsia* spp.), Manchurian Ash (*Fraxinus mandshurica* spp.), and Mongolian Oak (*Quercus* spp.) were purchased from the flooring retailers in China. One Poplar (*Populus* spp.) sample was cut from a disc of a 16-yr-old NL-6583 tree in China. Two oak (White Oak and Red Oak) samples were obtained from the discs of 75- and 45-yr-old trees (counted from pith to bark), respectively, in Knoxville, TN. Two samples for each species with sizes of 7 (T) × 17 (L) × 188 (R) mm for Red Oak; 7 (T) × 17 (L) × 179 (R) mm for White Oak, and 7 (T) × 17 (L) × 15 (R) mm for another eight hardwoods were prepared (Table 2). One specimen was for SilviScan and another one for nanoindentation tests. Therefore, the two specimens can be considered as coming from the same location of the tree for decreasing the position influence on the experiments.

For nanoindentation, one specimen with sizes of 2 (T) × 2 (R) × 5 (L) mm per each species was prepared using sharpened blades from nanoindentation samples, respectively, and were equilibrated to about 12% MC. The specimens were then embedded in epoxy resin, which was formulated by cycloaliphatic epoxide resin (ERL-4221; 2.5 parts), polycyclodiepoxide (DER-736; 1.5 parts), nonenyl succinic

Table 2. *Specimens dimension for microfibril angle measurement.*

Species	Tangential (mm)	Longitudinal (mm)	Radial (mm)
White Oak	2	7	179
Red Oak	2	7	188
Other eight species	2	7	15

anhydride (6.5 parts), and dimethylaminoethanol (0.1 parts). The embedded specimens were placed in a desiccator under vacuum for 12 h and then were cured in an oven at 70°C for 8 h. The cured specimens were cut and glued to acrylic blocks for microtoming. The specimens were then mounted onto an ultramicrotome and cut cross-sectionally with a glass knife. Finally, the specimen surface was cut by a diamond knife for obtaining a smoother surface. The smoothened specimens were conditioned in the nanoindentation test room for at least 24 h at 21°C ± 1°C and 60% ± 5% RH before the test was performed.

For SilviScan scanning, 10 hardwood specimens were further cut into final sizes listed in Table 2, then equilibrated to approximately 12% MC and scanned by an X-ray densitometry to determine the wood density (EvalueTree Technical Corp, Vancouver, Canada) at the Pulp and Paper Research Institute of Canada (Paprican, UBC Campus, Vancouver, BC, Canada). Ten thinner specimens with sizes as listed in Table 2 were then cut from the 10 samples for the measurement of microfibril angle by an X-ray diffractometry in the SilviScan system.

Nanoindentation Procedure

All nanoindentation experiments were performed by a Nano Indenter II (MTS System Corp., Oak Ridge, TN) equipped with a three-sided pyramid diamond indenter tip (Berkovich type) at the Oak Ridge National Laboratory (Oak Ridge, TN). The indentation experiment consisted of four segments (Fig 1). The first segment was the approach segment with an indenter surface approach rate of 10 nm/s. Once the tip contacted the specimen surface, a constant displacement rate of 5 nm/s was applied until a designed indentation depth of 200 nm was reached. At this depth, the maximum loading force was held for 30 s before the ultimate unloading. This holding segment was used for the thermal drift corrections. In the unloading segment, a constant displacement rate of 10 nm/s was applied until 90% of the maximum loading force was removed. At the end of
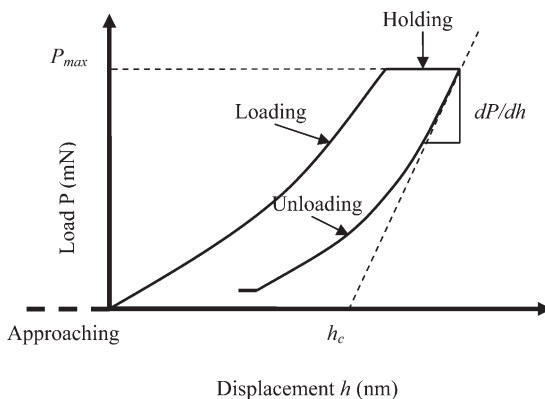

Figure 1.   Typical load displacement curve of a nanoindent.

experiment, the specimen was examined by the video system of the Nano Indenter II to evaluate the position and quality of the indents. Forty indents were made on five to nine latewood fiber tracheid cell walls for each specimen (Fig 2). In general, the S_2 layer comprises approximately 80% of the thickness of the cell walls. Thus, the properties of the S_2 layer determine the mechanical properties of the fiber tracheids. Accordingly, most indentation tests were performed on the S_2 layers with a few exceptions. For reliable data analysis, results taken from outside of the S_2 layer have to be
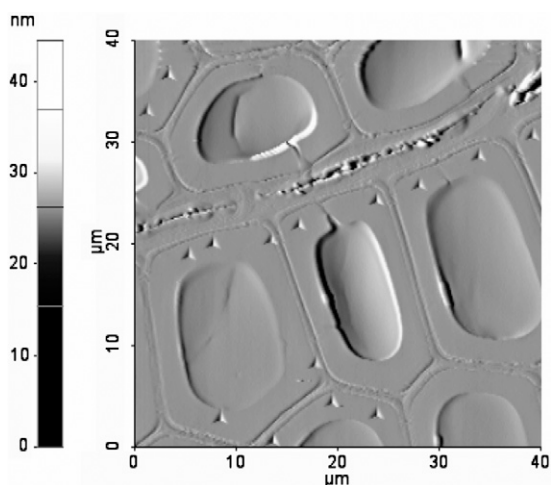

Figure 2.   Atomic force microscopy topography of Asian White Birch after nanoindentation.

eliminated. This also minimizes the edge effects on the determined cell wall properties.

On the basis of the theory of nanoindentation, the reduced modulus, E_r (the composite modulus for indenter and sample combination), can be evaluated from the nanoindentation measurements by using the following equation (Oliver and Pharr 1992):

$$E_r = \frac{\sqrt{\pi}\left(\frac{dP}{dh}\right)_{unloading}}{2\sqrt{A_{hc}}} \tag{1}$$

where P is the indentation load; h and h_c are the penetration and contact depths, respectively; and A_{hc} is the projected contact area, which is a function of the contact depth.

The Meyer hardness (H) can be obtained from the following equation:

$$H = \frac{P_{\max}}{A_{hc}} \tag{2}$$

The sample modulus (E_s) can be calculated as follows:

$$E_s = (1 - \nu_s^2)\left(\frac{1}{E_r} - \frac{1 - \nu_i^2}{E_i}\right) \tag{3}$$

where E_s is Young's modulus and ν_s is Poisson's ratio of the specimen; E_i and ν_i are the corresponding values of the indenter. For the diamond indenter used in our experiments, $E_i = 1141$ GPa and $\nu_i = 0.07$. Also, in all calculations, ν_s was assumed to be 0.25. From Eqs $1 - 3$, Young's modulus and the hardness of the cell wall of the fiber can be obtained.

Atomic Force Microscopy Scanning

After indentation was performed, the specimens were glued to the steel discs and mounted on the magnetic sample holder of the AFM XE-100 (PSIA Inc., Suwon, Korea) operated in contact mode. The surface of the specimens was scanned at a rate of 0.5 Hz and a set point of 24.73 nN. After atomic force microscopy scanning was performed, the topographies of the specimens were obtained at room temperature.

SilviScan Scanning

SilviScan is an automated wood microstructure analyzer developed for the rapid assessment of wood properties, including wood density and MFA, by a combination of X-ray diffractometry, X-ray densitometry, and digital microscopy (Evans 1997; Evans and Ilic 2001). The diffraction patterns collected on SilviScan can be integrated over the specified radial section; hence, pith-to-bark profiles of wood density and MFA variation can be obtained at different spatial resolutions. Density was scanned at a resolution of 25 μm, whereas MFA was in a resolution of 1 mm.

The elastic modulus of wood specimens can be calculated from the SilviScan wood density and MFA using the following equation:

$$E = A(DI_{CV})^B \tag{4}$$

where A and B are constants calibrated using sonic resonance data. D (kg/m^3) is the scanning wood bulk density and I_{CV} is the coefficient of variation of the 002 azimuthal diffraction profile determined by MFA (Evans 1999).

Statistical Analysis

One-way analysis of variance (ANOVA), linear regression, and parameter estimation analysis were conducted using Statistic Analysis System (SAS) JMP version 6.0.2 software (SAS Institute, Cary, NC). The SilvScan elastic modulus, microfibril angle, and wood density used for data analysis were all from the same tree ring in the specimen where the nanoindentation was done.

RESULTS AND DISCUSSION

Wood Properties Evaluated by SilviScan

The properties of 10 hardwoods are summarized in Table 3. The SilviScan elastic modulus of Keranji appeared to exhibit the highest value of 35.4 GPa, whereas poplar exhibited the lowest elastic modulus of 14.2 GPa. Moreover, the scanned wood density is the predominant factor

Table 3. *Wood properties of 10 hardwoods.*

Species	D_S (kg/m³)	E_N (GPa)	E_S (GPa)	H (GPa)	MFA (degree)
Poplar	478	16.9 (1.9)	14.2 (1.9)	0.49 (0.047)	15.8 (0.087)
Alder Birch	725	19.7 (1.1)	20.0 (2.1)	0.49 (0.032)	11.9 (0.061)
Asian White Birch	730	17.5 (2.1)	18.5 (2.3)	0.45 (0.033)	11.1 (0.057)
Red Oak	742	22.6 (1.5)	19.1 (1.6)	0.55 (0.037)	10.5 (0.047)
Iroko	786	22.9 (2.5)	16.1 (1.9)	0.51 (0.040)	9.70 (0.033)
White Oak	671	19.5 (1.8)	21.2 (2.4)	0.49 (0.028)	10.7 (0.032)
Manchurian Ash	570	18.5 (1.9)	14.5 (1.7)	0.48 (0.048)	12.0 (0.050)
Mongolian Oak	907	18.4 (2.0)	23.6 (4.3)	0.44 (0.047)	11.5 (0.054)
Kwila	892	21.2 (1.5)	24.4 (2.7)	0.56 (0.031)	2.80 (0.021)
Keranji	1187	24.6 (2.0)	35.4 (7.4)	0.54 (0.022)	5.90 (0.036)
Maximum	1187	24.6 (2.0)	35.4 (7.4)	0.56 (0.031)	15.8 (0.087)
Minimum	478	16.9 (1.9)	14.2 (1.9)	0.40 (0.028)	5.90 (0.036)
Mean	769	20.2 (1.8)	21.0 (2.8)	0.49 (0.037)	10.8 (0.051)
P (%)	59.7	31.3	59.9	28.6	62.7

Note: All data from one selected latewood. Ds, SilviScan density, D = M/V; M, V were the sample mass and volume at 12% MC; E_N, elastic modulus from nanoindentation; E_S, elastic modulus from SilviScan; H, hardness from nanoindentation; MFA, mean value of microfibril angle measured by SilviScan scanning; P, percentage of the difference between the maximum and minimum values. The numbers in the parentheses represent the SD.

that determines the SilviScan elastic modulus. The higher the scanned wood density, the higher the SilviScan elastic modulus. The scanned density of hardwood can be affected by either thickening of the dense cell walls to decrease the void volume or filling of some other substances with lower density in the lumen or vessels such as gelatinous layer (G-layer), tyloses, and gummy substance in vessels. Thus, the more the substances with lower density are clogged in the voids, the higher the scanning wood density. The extreme high scanned elastic modulus species were Kwila and Keranji. The thick G-layer in Kwila wood as seen in Fig 3 obtained by environmental scanning electron microscopy was the main contributor to the higher scanned elastic modulus. G-layer is an obvious characteristic of tension wood in hardwoods, which indicates that Kwila in this study was a tension wood, not a normal wood. Thus, it was excluded in the following regression analysis and only nine hardwoods were compared.

The ANOVA test showed that the effect of wood density on the SilviScan elastic modulus was highly significant at a confidence level of 95% ($P = 0.0003$). A linear regression analysis ($R^2 = 0.85$) indicated that the SilviScan elastic modulus increased with wood density as shown in Fig 4. The parameter estimation test showed that
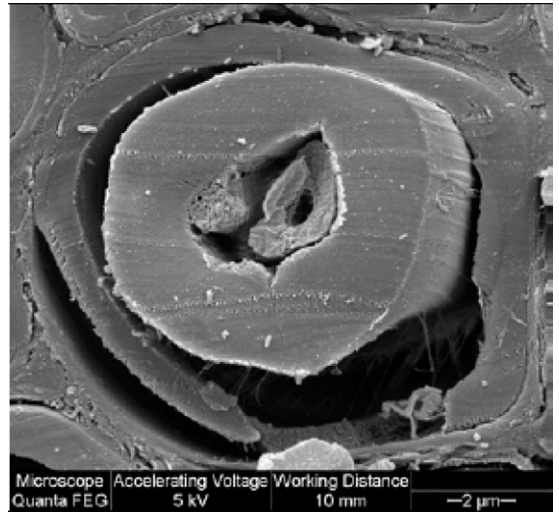

Figure 3. High resolution environmental scanning electron microscopy image of a G-layer in the fiber lumen of Kwila wood (taken by environmental scanning electron microscopy in Canada).

the effects of parameter *x* (wood density) in the linear regression equation were highly significant, whereas the intercept was not significant on *y* (SilviScan elastic modulus). This indicates that wood density is the predominant factor that determines the SilviScan elastic modulus.

Another important contributor to the SilviScan elastic modulus is MFA. The ANOVA test showed that the effect of MFA on the SilviScan
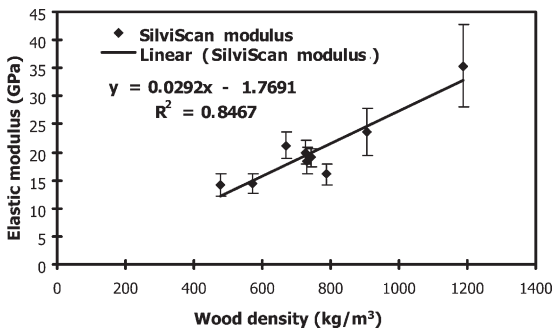
Figure 4. Relationship between SilviScan elastic modulus and wood density.
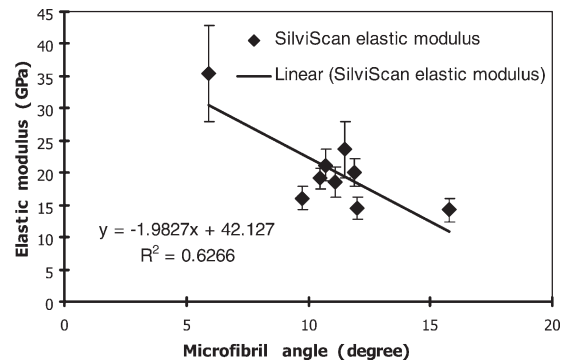

Figure 5. Relationship between SilviScan elastic modulus and microfibril angle (MFA).
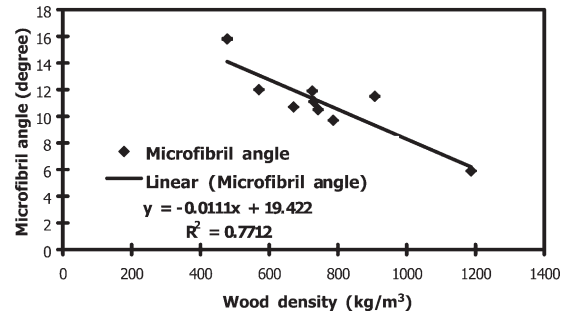
Figure 6. Relationship between microfibril angle and wood density.

elastic modulus was significant ($P = 0.015$). A decreasing tendency was observed in the Silvi-Scan elastic modulus with increasing MFA as shown in Fig 5. A regression analysis ($R^2 = 0.63$) indicates that a linear relationship exists between SilviScan elastic modulus and MFA. This agreed with the findings that the longitudinal stiffness and effective modulus decreased with increasing MFA, as reported by Harrington et al (1998), Gindl and Schöberl (2004), and Tze et al (2007). However, the parameter estimation revealed that the effect of intercept ($P = 0.00006$) in the linear regression equation on y (SilviScan elastic modulus) was more highly significant than that of parameter x (MFA) ($P = 0.015$). This indicates that MFA is not the first contributor to the SilviScan elastic modulus system.

A linear relationship ($R^2 = 0.77$) was observed between MFA and wood density as seen in Fig 6. This indicates that lower density wood species have higher MFA than higher density wood species.

Wood Properties Evaluated by Nanoindentation

The nanoindentation test focuses on the individual wood cell wall. The test results represent the natural properties of fiber cell wall, not the whole wood. Thus, nanoindentation results should be more referable when the nature of fiber properties is considered. As listed in Table 3, the highest cell wall elastic modulus of 24.6 GPa was observed in Keranji, which was

lower than its SilviScan modulus (35.4 GPa). It should be noted that SilviScan modulus and nanoindentation modulus are different measurements of mechanical properties. The very high density proves that the proportion of voids in Keranji wood is very limited and the principal substance in the wood is cell wall materials. The lowest elastic modulus of 16.9 GPa was observed in Poplar. The percentage of the difference in elastic modulus between Keranji and Poplar was 31.3%. According to the findings of Kellogg and Wangaard (1969), the cell wall density among 18 species of hardwoods and softwoods varied from 1497 – 1529 kg/m^3. The variation was very limited. This indicates that the higher difference of elastic moduli by nanoindentation is not only the result of the cell wall density. The MFA, the cell wall components and its microstructures, the visco-elastic effects, the creep behavior during

nanoindentation, and other inevitable artifacts could be contributors. The influence of cell wall thickness, ie the neighboring effect during the nanoindentation test, could also be an important factor to be noticed. If the indent size is not small enough, the values of nanoindentation elastic modulus in thinner wood cell wall species can be affected by the neighboring materials with lower density (such as epoxy resin), and therefore a lower experimental value is obtained. This indicates that for the evaluation of thinner cell wall fibers, the indent size must be small enough to reduce the neighboring effect of the embedding resin. For improving the reliability of the nanoindentation results of wood cell walls, it is necessary to have tight control of the nanoindentation procedure and analysis of the load displacement data.

A linear regression analysis ($R^2 = 0.49$) showed that wood cell wall elastic modulus increased with wood density. However, the parameter estimation revealed that the effect of intercept ($P = 0.0002$) in the linear regression equation on y (wood cell wall elastic modulus) was more highly significant than that of parameter x (wood bulk density) ($P = 0.0075$). This indicates that another factor other than bulk density of wood contributes to the cell wall elastic modulus.

As shown in Fig 7, wood cell wall elastic modulus decreased with increasing its MFA that was taken from the same tree ring in the specimen. A linear regression analysis showed the relationship
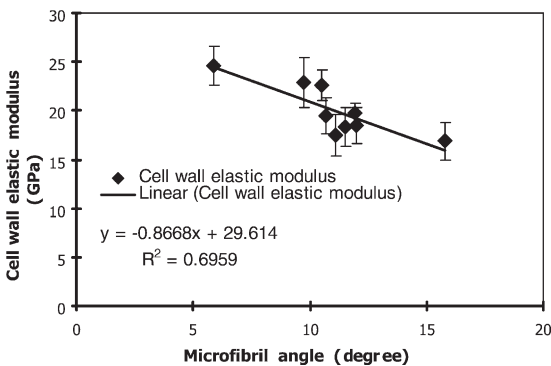

Figure 7. Relationship between cell wall elastic modulus and microfibril angle (MFA).

that existed between MFA and the cell wall elastic modulus ($R^2 = 0.70$). This decreasing trend of elastic modulus with increasing MFA agreed with the results of other researchers (Harrington et al 1998; Gindl and Schöberl 2004; Tze et al 2007). The parameter estimation revealed that the effect of intercept ($P = 0.0001$) in the linear regression equation on y (wood cell wall elastic modulus) was more highly significant than that of parameter x (MFA) ($P = 0.0020$). This also proved that the cell wall elastic modulus was influenced by multiple factors such as the complex wood cell wall structures and components.

The values of hardness of cell wall varied from 0.44 – 0.56 GPa. There was no distinct difference from the values of softwoods (0.34 – 0.54 GPa) reported by Gindl and Schöberl (2004) and Tze et al (2007). According to macroscopic wisdom, hardness in softwoods was higher than that in hardwoods (Yin 1996), but in this study at the nanometer scale, the distinct difference was not observed. In general, higher bulk density of wood always relates to higher hardness in bulk wood (Yin 1996). However, this trend was not found in the cell wall hardness. The ANOVA test also revealed that there was no significant difference in hardness among 10 species ($P = 0.1$).

The relationship between cell wall hardness and MFA was also investigated. It appeared that there was no obvious tendency between cell wall hardness and MFA. This seems to be contradictory to the results of Gindl and Schöberl (2004) and Tze et al (2007). This could be attributed to the fact that the MFA was not the major variable to hardness among species and it has been demonstrated to vary depending on the location within the tree (height), growth ring, cardinal direction within the tree, and type of wood, namely, mature wood, juvenile wood, and reaction wood.

CONCLUSIONS

The following conclusions can be drawn from this study. The elastic moduli evaluated by SilviScan of 10 hardwoods were significantly different among species. The SilviScan elastic modulus increased with increasing wood density and decreased with increasing microfibril

angle. Lower density hardwood species exhibited higher MFA than higher density species. At the cell wall level, the elastic modulus and hardness obtained by nanoindentation were more related to the properties of natural fibers. The difference in cell wall elastic modulus among the species was significant, whereas the difference in hardness was insignificant.

REFERENCES

Cave ID (1968) The anisotropic elasticity of the plant cell wall. Wood Sci Technol 24:268 – 278.

——— (1969) The longitudinal modulus of *Pinus radiata*. Wood Sci Technol 3:40 – 48.

Cheng J, Yang J, Liu P (1992) Wood science records. China Forestry Publishing Company. Beijing. Pages 697 – 698 (in Chinese).

Cheng Q, Wang S, Rials TG, Lee SH (2007) Physical and mechanical properties of polyvinyl alcohol and polypropylene composite materials reinforced with fibrils isolated from regenerated cellulose fibers. Cellulose 14(6):593 – 602.

Chudnoff M (1979) Tropical timbers of the world. USDA For Prod Lab, Madison, WI. 831 pp.

Cown DJ, Herbert J, Ball RD (1999) Modelling *Pinus radiate* lumber characteristics. Part 1: Mechanical properties of small clears. N Z J Sci 29:203 – 213.

Evans R (1997) Rapid scanning of microfibril angle in increment cores by X-ray diffractometry. Pages 116 – 139 *in* BG Butterfield, ed. Microfibril angle in wood. Proc IAWA/IUFRO International Workshop on the Significance of Microfibril Angle to Wood Quality. University of Canterbury Press, Westport, New Zealand.

——— (1999) A variance approach to the X-ray diffractometric estimation of microfibril angle in wood. Appita J 51:53 – 57.

———, Ilic J (2001) Rapid prediction of wood stiffness from microfibril angle and density. Forest Prod J 51 (3):53 – 57.

Fengel D, Stoll M (1973) Über die Veränderung des Zellquerschnitts, der Dicke der Zellwand und der Wandschichten von FichtenholzTracherden innerhalb eines Jahrrings. Holzforschung 27:1 – 7.

Forest Products Laboratory (1999) Wood handbook—Wood as an engineering material. Gen. Tech. Rep. FPL-GTR-113. USDA Forest Products Laboratory, Madison, WI. 463 pp.

Gindl W, Schöberl T (2004) The significance of the elastic modulus of wood cell walls obtained from nanoindentation measurements. Compos Part A-Appl S 35:1345 – 1349.

Gordon JE, Jeronimidis G (1980) Composites with high work of fracture. Phil Trans Res Soc London 294:545 – 550.

Harrington JJ, Booker R, Astley RJ (1998) Modelling the elastic properties of softwood. Part I: The cell-wall lamellae. Holz Roh Werkst 56:37 – 41.

Holmberg H (2000) Influence of grain angle on Brinell hardness of Scots pine (Pinus sylvestris L.). Holz Roh Werkst 58:91 – 95.

Jentzen CA (1964) The effect of stress applied during drying on some of the properties of individual pulp fibers. Tappi J 47:412 – 418.

Jiang ZH, Yu Y, Fei BH, Ren HQ, Zhang TH (2004) Nanoindentation technique testing the longitudinal elastic modulus and hardness in tracheid secondary S_2 layer. Scientia Silvae Sinicae 4(2):113 – 118 (in Chinese).

Keller A (2003) Compounding and mechanical properties of biodegradable hemp fiber composites. Comp Sci Technol 63(9):1307 – 1316.

Kellogg RM, Wangaard FF (1969) Variation in the cell-wall density of wood. Wood Fiber Sci 1(3):180 – 204.

Kollman FFP, Côté WA (1968) Principles of wood science and technology, Vol I. Springer-Verlag, New York, NY. 592 pp.

Lee S, Wang S, Pharr G, Kant M, Penumadu D (2007) Mechanical properties and creep behaviour of lyocell fibers by nanoindentation and nano-tensile testing. Holzforschung 61(3):254 – 260.

Meylan BA, Butterfield BG (1978) Helical orientation of the microfibril in tracheids, fibres and vessels. Wood Sci Technol 12:219 – 222.

Miyajima H (1963) Studies in the indentation hardness of wood. Res Bull For Hokkaido University 22(2):539 – 607.

Mohanty AK, Misra M, Drzal LT (2001) Surface modifications of natural fibers and performance of the resulting biocomposites: An overview. Compos Interface 8(5):313 – 343.

Nilsson T, Gustafsson PJ (2007) Influence of dislocations and plasticity on the tensile behaviour of flax and hemp fibres. Compos Part A-Appl S 38:1 – 30.

Oliver WC, Pharr GM (1992) An improved technique for determining hardness and elastic modulus using load and displacement sensing indentation experiments. J Mater Res 7:1564 – 1583.

Shibata M, Oyamada S, Kobayashi S, Yaginuma D (2004) Mechanical properties and biodegradability of green composites based on biodegradable polyesters and lyocell fabric. J Appl Polym Sci 92:3857 – 3863.

Tze WT, Wang S, Rials TG, Pharr GM, Kelley SS (2007) Nanoindentation of wood cell wall: Continuous stiffness and hardness measurements. Compos Part A-Appl S 38:945 – 953.

Wang S, Lee SH, Tze WT, Rials TG, Pharr GM (2006) Nanoindentation as a tool for understanding nano-mechanical properties of cell wall and biocomposites *in*

International Conference on Nanotechnology for the Forest Products Industry, Marriott Marquis, Atlanta, GA. 7 pp.

Xing C, Wang S, Pharr GM (2009) Nanoindentation of juvenile and mature loblolly pine (*Pinus taeda L.*) wood fibers as affected by thermomechanical refining pressure. Wood Sci Technol (accepted).

———, ———, ———, Groom L (2008) Wood fiber properties affected by thermomechanical refining steam pressure using nanoindentation. Holzforschung 62(2): 230 – 236.

Yin S (1996) Wood science. China Forestry Publishing Company, Beijing, China. 176 pp (in Chinese).

Ylinen A (1943) Über den Einfluß der Rohwichte und des Spätholzanteils auf die Brinellhärte des Holzes. Holz Roh Werkst 6(4):125 – 127.

Zini E, Baiardo M, Armelao L, Scandola M (2004) Biodegradable polyesters reinforced with surface-modified vegetable fibers. Macromol Biosci 4:286 – 295.